Colloids and Surfaces A: Physicochemical and Engineering Aspects 681 (2024) 132838

Contents lists available at ScienceDirect

Colloids and Surfaces A: Physicochemical and Engineering Aspects

journal homepage: www.elsevier.com/locate/colsurfa

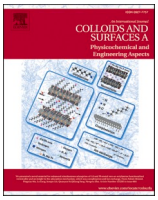

Role of hydrodynamic conditions and type of foam stabilizer for antifoam efficiency

V. Georgiev [a], Z. Mitrinova [a], A. Gers-Barlag [b], G. Jaunky [b], N. Denkov [a], S. Tcholakova [a,*]

[a] Department of Chemical Engineering, Sofia University, Sofia, Bulgaria
[b] BYK Chemie, Germany

GRAPHICAL ABSTRACT

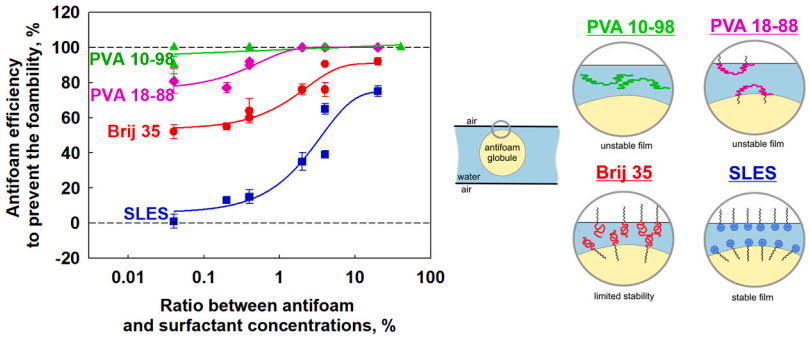

ARTICLE INFO

Keywords:
Foams
Polyvinyl alcohol
Antifoam compound
Antifoam emulsion
Foaming tests

ABSTRACT

The effects of antifoam and surfactant concentration on the foamability of solutions of an anionic (SLES) and nonionic (Brij 35) surfactants and a series of polyvinyl alcohols with 88% and 98% degree of hydrolysis and molecular masses between 31 and 205 kDa, were studied. Three methods which differ in the way of air incorporation were used for foaming – Bartsch test, shake test and Ultra Turrax. Mixed silicone oil-silica particles antifoam was studied. The antifoam was introduced in the foaming solution as pre-dispersed in organic solvent or as antifoam-in-water emulsion. It was shown that the antifoam is very active in the fast foaming methods (Bartsch and shake tests) for the slow adsorbing polymers PVA and has no any activity in the slow foaming method (Ultra Turrax) for the fast adsorbing surfactants with electrostatic stabilization (SLES). The efficiency of pre-dispersed in organic solvent antifoam is much higher as compared to that of emulsified antifoam, due to the faster segregation of the silica particles and silicone oil in the emulsified antifoam. The antifoam efficiency increases with antifoam concentration and with lowering the surfactant concentration. In a given foaming method, the antifoam efficiency is the highest in PVA solutions with 98% DH, intermediate for PVA with 88% DH and Brij 35, and the lowest for SLES solutions. At a certain degree of hydrolysis, the molecular mass of PVA has no significant effect on the antifoam activity. Good correlation between the antifoam efficiency and the stability of the pseudo emulsion film formed between the antifoam globule and the bubble surface is established, showing

* Correspondence to: Department of Chemical and Pharmaceutical Engineering, Faculty of Chemistry and Pharmacy, Sofia University, 1 James Bourchier Ave., 1164 Sofia, Bulgaria.
E-mail address: SC@LCPE.UNI-SOFIA.BG (S. Tcholakova).

https://doi.org/10.1016/j.colsurfa.2023.132838
Received 19 October 2023; Received in revised form 16 November 2023; Accepted 20 November 2023
Available online 22 November 2023
0927-7757/© 2023 The Author(s). Published by Elsevier B.V. This is an open access article under the CC BY-NC-ND license (http://creativecommons.org/licenses/by-nc-nd/4.0/).

that the electrostatic repulsion is more efficient to prevent the entering of the antifoam globules on the air-water interface, as compared to the steric repulsion.

1. Introduction

The ability of home and personal products to generate foam is very important for consumer perception during their application [1–4]. In many applications the requirements are for good foamability during the application stage and fast foam destabilization during the rinsing stage to decrease the water consumption. The control of bubble stability is important also for fabrication of nanoparticles [5], alkaline water electrolysis [6], nanotube formation [7], etc. There are a lot of applications in which the foams are undesired and defoamers or antifoams are added to prevent or control the foamability, such as oil and gas production [8–12], fermentation [13–15], paper production [16–19], textile dying [20], laundry washing products [21,22], painting [23–25], etc. Typical antifoams contain hydrophobic particles, oil or their mixtures [26–30]. The mixed antifoams (mixture of hydrophobized particles and liquid oil) destroy the foams via bridging-stretching or/and bridging-dewetting mechanisms [29,30].

Denkov et al. [31] showed that depending on the mechanism of their action, three different types of antifoam can be distinguished: fast, slow and dynamic. Fast antifoams disrupt the foam films during thinning, typically leaving no residual foam at approx. 30 s after stopping the agitation [30,31]. These antifoams are able to enter on the bubble surfaces at very low compressing pressures, at less than 15 Pa, and to form oil bridges between the opposite foam film surfaces [32,33]. These bridges rapidly stretch and rupture, inducing foam collapse [32]. The slow antifoams need much higher compressing pressure for entering the air-water interface, therefore, the antifoam globules are expelled from the foam films and accumulate in the Plateau channels [31]. During the water drainage from the foam these globules become compressed and enter the air-water interface, where the oil spreads and induces breakage of the neighboring foams films [34]. Dynamic antifoams disrupt foams only during foam generation, when the surfactant adsorption layers are far from equilibrium and the antifoam globules can easily penetrate the air-water interface due to the lower stability of the pseudo-emulsion film formed between the globule and the bubble surface [35].

In our previous study [36] we showed that the action of silicone-silica antifoam, acting under dynamic conditions, depends strongly on the antifoam concentration and on the area per molecule in the adsorption layers formed on the bubble surface. Formation of dense adsorption layer leads to low activity of the studied antifoam, due to the higher barrier for entering the antifoam globules on the bubble surface during foaming. This entry barrier depends on the stability of the film formed between the antifoam globule and the bubble surface, which can be significantly decreased by the solid hydrophobic particles in mixed antifoams [31]. Marinova & Denkov [37] showed that the activity of dynamic antifoams depends very significantly on the procedure by which the antifoam globules are introduced in the foaming solution – better activity is determined for antifoam emulsions as compared to antifoam compounds for foams stabilized by alkyl polyglycoside (APG) surfactant. This effect was explained with the larger protrusion depth of the solid Span particles used for stabilization of the antifoam emulsion, as compared to the silica particles which were present in both formulations - antifoam compound and antifoam emulsion. Larger protrusion depth is required to break the pseudo-emulsion film and induce globule entry, because APG forms relatively thick films with thickness of ≈ 100 nm [37].

It is known from the literature that polymers adsorbing on the film surface induce long range steric repulsion between them, and as a consequence, the formed films are thicker as compared to the films stabilized by low molecular mass surfactants [38–43]. On the other hand, the ability of polymer surfactants to reduce the dynamic surface tension is much lower as compared to low molecular mass surfactants [44]. Therefore, it is not clear in advance which of these two factors will be more important for the antifoam action of mixed antifoams.

Polyvinyl alcohols are hydrophilic polymers that are used for surface modification of paper [45], formation of nanocomposites [46–48], preparation of different medical devices [49,50], etc. Recently we showed that the foamability of PVA solutions depends on the PVA concentration, the degree of hydrolysis and the method used for foam generation [44]. In our recent studies [44,51,52] we showed that, depending on the nature of surfactant used, three different master curves are obtained when the foamability (in absence of antifoam) is plotted as a function of the instantaneous surface coverage of the bubbles by surfactants: (1) For anionic surfactant in which long range electrostatic repulsion acts between film surfaces, the foamability starts to increase at very low surface coverage of ≈ 20%; (2) For nonionic surfactants where only short range steric repulsion is important for foam film stabilization a steep increase in the foamability is observed at surface coverage of ≈ 95%; (3) For PVA solutions which induce long range steric repulsion, the increase in foamability starts at a surface coverage of ≈ 80%. It is not clear in advance how those three types of foam stabilization affect the antifoam action of the mixed antifoams.

The major aims of the current study are: (1) To investigate the antifoam efficiency with respect to the foamability of anionic (SLES), nonionic (Brij 35) and PVA with 88% and 98% degrees of hydrolysis (DH) at different antifoam and surfactant concentrations; (2) To determine the effect of hydrodynamic conditions on the antifoam activity by comparing the antifoam efficiency in three different foaming methods – fast foaming method (Bartsch test) and two methods with intermediate rate of expansion of the bubble surface during foam generation, while being with very different way of air incorporation – Ultra Turrax and shake test; (3) To compare the efficiency of antifoams introduced in the foaming solution as antifoam dispersion in solvent or as antifoam emulsion stabilized by Tween/Span mixture.

2. Materials

For performing the experiments in the current study, we used the materials described in detail in Ref. [44]: anionic sodium lauryl ether sulfate (SLES), non-ionic polyoxyethylene-23 lauryl ether (Brij 35), and polyvinyl alcohols (PVA) with different molecular weights (M_W) between 27 and 205 kDa and two different degrees of hydrolysis (DH) of 88% and 98%. The PVA samples are products of Sigma-Aldrich. The acronyms used in the text are PVA 4–98 (M_W = 27 kDa; 98% DH); PVA 10–98 (M_W = 61 kDa; 98% DH); PVA 4–88 (M_W = 31 kDa; 88% DH); PVA 8–88 (M_W = 67 kDa; 88% DH); PVA 18–88 (M_W = 130 kDa; 88% DH); PVA 40–88 (M_W = 205 kDa; 88% DH). The procedures for solution preparation are described in detail in Ref. [44].

The studied antifoam is a mixture of polyether modified silicone oil and hydrophobized silica particles. The antifoam was introduced in the foaming solutions by two different ways: (1) As pre-dispersed mixture in solvent 2,2,4-Trimethyl-1,3-pentanediol diisobutyrate (TXIB, Sigma-Aldrich, cat.: 525170) or as (2) Emulsified antifoam in the form of oil-in-water emulsion which is stabilized by Span/Tween mixture. For preparation of antifoam dispersion, a certain amount of AF is added in to TXIB and homogenized for 15 min on a magnetic stirrer to obtain antifoam dispersion with concentration between 2 and 20 wt%. This stock dispersion is employed afterwards for introducing the antifoam component into the foaming solution at the desired final concentration. Throughout the text, the outcomes achieved through the utilization of the antifoam dispersion in TXIB for antifoam dosage within the foaming solution, are denoted as AFD (AntiFoam Dispersion).

For stabilization of antifoam-in-water emulsions we used a mixture of Span/Tween and thickeners. The prepared emulsions contained 20 wt % AF. When the antifoam is introduced as antifoam emulsion, it is denoted in the text as AFE. The microscopic observation of the studied emulsion showed that it is polydisperse with a drop diameter ranging from ca. 1–60 μm, see Fig. S1 in supporting information.

For both AFD and AFE, the concentration of the actual mixed AF is calculated and presented in the text. For example, when 1 g/L antifoam emulsion was added in the foaming solution, this corresponds to and is denoted in the text as 0.2 g/L antifoam concentration.

For foaming experiments the AF dispersion or AF emulsion were dosed in the foaming solutions from the top by using a micropipette (Eppendorf® Multipette® M4). The AF concentration was varied between 2 and 2000 ppm.

3. Methods

3.1. Spreading ability

The ability of the studied AFD and AFE to spread on the solution surface was determined by Wilhelmy plate method and by optical observation of the solution interface in reflected light. For determination of the spreading ability by Wilhelmy plate method we used K100 tensiometer (Kruess, Germany). Initially the surface tension of solution without antifoam was measured for 200 s at 25 °C. Afterwards a drop of AF was introduced onto the interface by using a needle and the surface tension measurement continued for at least additional 200 s. The spreading ability was determined from the drop of the surface tension after AF addition.

For optical observation of the spreading, a Petri dish with the studied foaming solution is placed on the table of optical microscope Axioplan (Zeiss, Germany), equipped with a long-distance objective Zeiss Epiplan 20 × /0.40, CCD camera (Sony SSC-C370P) and 5.1 M Video Biological Microscope Digital Camera 55FPS LCMOS. The observations are performed in reflected light. After a placement of AF drop on the solution surface the process of spreading starts. The observations are performed within 2 min after adding an antifoam drop on the solution surface.

3.2. Thin foam films in the presence of antifoams

The behaviour and stability of foam films formed from solutions shaken in Bartsch test, containing 200 ppm AF, introduced as AF dispersion or AF emulsion, were observed in the capillary cell of Scheludko-Exerowa [53]. The films were formed in a capillary with radius $R = 1.5$ mm by sucking out the solution through a side orifice and then were observed in reflected light with optical microscope Axioplan (Zeiss, Germany), equipped with a long-distance objective Zeiss Epiplan 20 × /0.40, CCD camera (Sony SSC-C370P) and H-264 Digital Video Recorder. The typical radius of the foam films formed in this capillary was $R_F \approx 0.15$ mm. The presence of antifoam in the solution affects the stability and the pattern of the film thinning.

3.3. Vertical foam films

The stability of vertical foam films was also studied for foaming solutions containing 200 ppm antifoam dispersion by using the experimental set-up described in Ref. [44].

3.4. Foam tests for foam formation and stability

In the present study three different foaming methods were studied: Bartsch test, Shake test and Ultra Turrax. They are characterized by different time scale for bubble formation, hydrodynamics and conditions for bubble collisions which could eventually lead to bubble coalescence and foam collapse [44].

The Bartsch test is characterized with the most vigorous shaking and significant surface expansion during the process of air entrapment. The method consists of 1000 shakes of 120 ml glass cylinder, containing 10 ml surfactant solution and a certain amount of antifoam. The foam volume was accounted first on every 10 cycles up to 200 cycles, then on every 50 cycles up to 1000 cycles.

In the Shake test the amplitude and the respective surface deformation are smaller. In this experiment 20 ml solution is placed in 50 ml plastic tubes which are shaken at 700 rpm for 1000 s and the foam volume was accounted first on every 10 s up to 200 s and then on every 50 s up to 1000 s

Stirring with T25 digital Ultra-Turrax, equipped with S 25 N-18 G rotational tool, ensures the the smallest surface deformation. 20 ml solution is filled in a 100 ml glass cylinder and is stirred at 20 000 rpm for 120 s. The foam volume was measured after 30 s (initial), 60 and 120 s (final). All foaming experiments were performed at 25 ± 0.5 °C.

In all experiments the antifoam dispersion or antifoam emulsion is added on the top of the foaming solution before starting the foaming test.

4. Experimental results from foaming experiments

In this section the experimental results about the antifoam efficiency with respect to the studied anionic SLES, nonionic Brij 35, polymeric PVA solutions with 88% DH and different molecular masses (PVA 4–88; PVA8–88; PVA 18–88 and PVA 40–88) as well as of PVA solutions with 98% DH (PVA 4–98 and PVA10–98) are presented for foams formed in Bartsch test (Section 4.1); shake test (Section 4.2) and in Ultra Turrax (Section 4.3). The results obtained in the different tests are compared in Section 4.4.

4.1. Bartsch test

In the first series of experiments the antifoam concentration was varied between 2 and 200 ppm at fixed surfactant concentration of C_S = 5 g/L. The antifoam was introduced in foaming solutions as a dispersion in TXIB (AFD) or as an antifoam emulsion (AFE). The obtained results for the foamability as a function of the number of shaking cycles, n, are shown in Figs. S2 and S3 in Supporting information. For all studied surfactants and PVAs, the addition of AF in the foaming solution leads to significant decrease in its foamability during the whole period of foam generation.

The antifoam efficiency, AE, is defined as a ratio between the volume of destroyed foam in the presence of antifoam and the volume of the foam which is generated without antifoam added to the same foaming system. The percentage of remaining foam, RF, is defined as the ratio between the volume of generated foam in the presence of antifoam, V_A(+AF), and that generated in absence of antifoam, V_A(no AF):

$$AE = 1 - RF;\ RF = V_A(+AF)/V_A(\text{no AF}) \quad (1)$$

The values of AE and RF varied between 0% and 100%. Higher value of RF means lower antifoam efficiency and vice versa. The dependence of RF on n for solutions containing different concentrations of antifoam, introduced as AFD or AFE, are shown in Figs. S4 and S5. For most PVA solutions, RF remains almost constant for all n, showing that the AF remains very active during all 1000 shaking cycles. The gradual increase of RF with n, observed for SLES and Brij 35 solutions, show that the antifoam efficiency decreases upon increasing the number of shaking cycles. This effect is related to some exhaustion of the AF during the foaming process, due to the segregation of the silica particles and silicone oil, as shown in Ref. [54]. The observed slower exhaustion of AF in PVA solutions is related to the different spreading behavior as seen under the microscope and different antifoam efficiency of silicone oil without silica particles (Section 5 below).

To compare the efficiency of the studied antifoam with respect to different surfactant and polymer solutions, we determined the value of

AE after 10; 100 and 1000 shaking cycles and compared them in Fig. 1. It is seen that $AE = 100\%$ for all shaking cycles and antifoam concentrations for PVA solutions with 98% DH. For these solutions even, addition of 2 ppm AF dosed as AFD is sufficient to destroy completely the foam. After 10 shaking cycles $AE = 20\%$ for SLES stabilized foam at $C_{AF} = 2$ ppm and increases up to 70% at $C_{AF} = 200$ ppm. For Brij 35 and PVA with 88% DH, $AE \approx 70\%$ at $C_{AF} = 2$ ppm and becomes almost 100% at $C_{AF} = 20$ ppm after 10 shaking cycles. Upon prolonged shaking, *AE* decreases for SLES and Brij 35, but remains constant for PVA with 88% DH. As a consequence, after 1000 cycles $AE \approx 0\%$ for SLES solution at $C_{AF} = 2$ ppm, which means that the antifoam had been exhausted and the volume of entrapped air after 1000 cycles is the same for solutions with and without antifoam. Due to the exhaustion of antifoam in Brij solution, the curve for *AE* vs C_{AF} after 1000 cycles lay below the curve for PVA solutions with 88% DH, whereas after 10 shaking cycles they are very close to each other, see Fig. 1. From these experiments we can conclude that the efficiency of the AF is the highest for PVA with 98% DH, intermediate for PVA with 88%DH and Brij 35, and the lowest for SLES solutions. The efficiency of antifoam increases with C_{AF} and decreases with *n* for low molecular mass surfactants (SLES and Brij 35) and does not depend on *n* for PVA solutions.

The experimental data for *AE* vs C_{AF} after 10; 100 and 1000 shaking cycles for solutions in which AF is introduced as aqueous emulsion are shown in Fig. S6. As can be seen, *AE* increases almost linearly with $\lg C_{AF}$ for most of the studied systems. The efficiency of AF introduced as antifoam dispersion is better as compared to its efficiency when it is introduced as antifoam emulsion with respect to the sterically stabilized foams (PVA and Brij 35), see Fig. 2. The effect is very significant for Brij35 for all studied AF concentrations and noticeable for PVA18–88, especially at low AF concentrations. When emulsified AF is used at the lowest $C_{AF} = 2$ ppm, not all of the bubbles are destroyed in the presence of AFE even in solutions of PVA with 98% DH. The lower efficiency of AF from AFE, as compared to AFD, especially at $C_{AF} = 2$ ppm is related to the easier segregation of the silica particles from the silicone oil in the course of oil spreading, see Section 5 below. This segregation leads to formation of silica-enriched and silica-free globules both of them with lower efficiency to destroy the foam. It is important also to note that the formation of antifoam emulsions requires the use of emulsifiers which adsorb on the drop surfaces. These emulsifiers could stabilize the pseudo-emulsion film that is formed between the antifoam drop and the air-water interface and thus to increase the entry barrier for the antifoam globules. Note that Span surfactants are known to form mixed adsorption layers with Brij 35 and this is used in the practice to prepare stable emulsions. The formation of such mixed adsorption layers also decreases the efficiency of the antifoam globules. The increase of C_{AF} leads to significant increase in the probability for entrapment of active antifoam globules in the foam films and thus to increase the ability of antifoam to induce bubble coalescence. Interestingly, in the initial stages of foam generation, better antifoam efficiency of AFE is determined as compared to AFD with respect to SLES foams. This effect is probably related to the different mode of antifoam spreading, see Section 5 below, and the possible formation of mixed adsorption layer between SLES and the nonionic surfactants coming from the emulsions, thus facilitating the foam destruction. Note that the latter effect is more pronounced at higher AF concentration which means also higher nonionic surfactant concentration in the foaming solution. The difference in the efficiency of AFE and AFD with respect to SLES foams disappears after 1000 cycles, whereas it remains significant for the nonionic surfactant and PVA

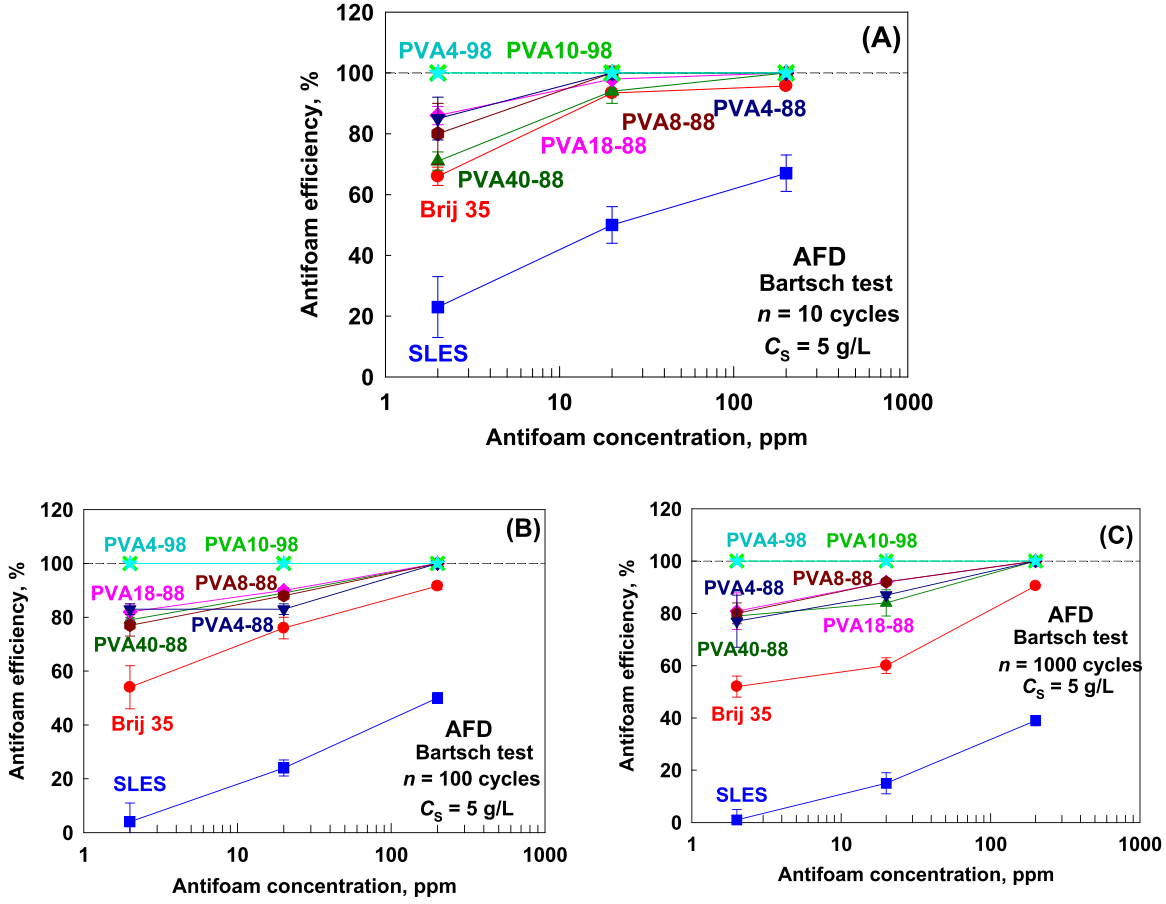

Fig. 1. Antifoam efficiency, *AE*, to destroy the foam generated after (A) 10; (B) 100 and (C) 1000 shaking cycles in Bartsch test from 5 g/L solutions of SLES (blue squares); Brij 35 (red circles); PVA 40–88 (green triangles up); PVA 18–88 (pink diamonds); PVA 8–88 (brawn hexagons); PVA 4–88 (blue triangles down); PVA 10–98 (green stars) and PVA 4–98 (cyan X) at different antifoam concentrations in which the antifoam is dosed as antifoam dispersion.

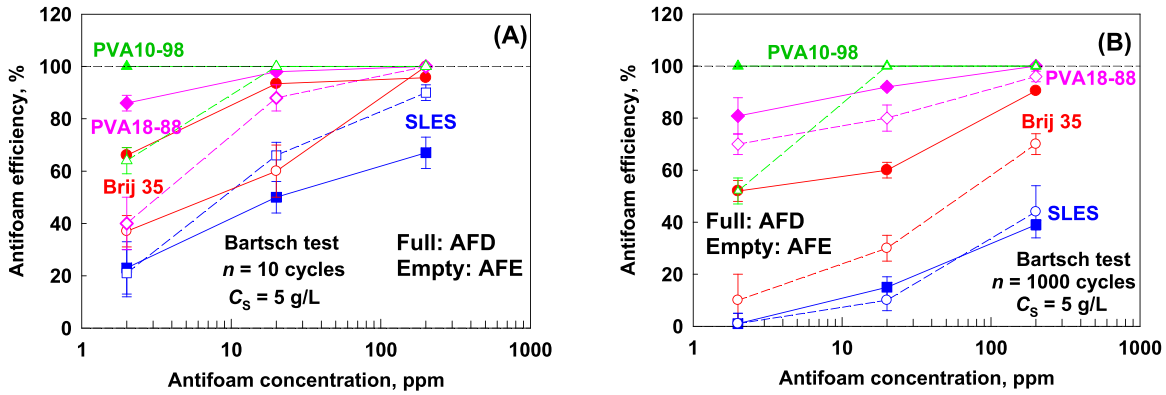

Fig. 2. Antifoam efficiency, *AE*, as a function of antifoam concentration, $C_{AF,}$ after (A) 10 and (B) 1000 cycles in Bartsch test for antifoam dosed as AFE (empty points) and AFD (full points) in 5 g/L solution of SLES (blue squares); Brij 35 (red circles); PVA 18–88 (pink diamonds); PVA 10–98 (green triangles).

solutions.

In the second series of experiments the effect of surfactant concentration was studied at fixed $C_{AF} = 20$ ppm for SLES, Brij 35 and PVA 18–88 solutions. The obtained results for the volume of entrapped air V_A vs. C_S at $n = 10$; 100 and 1000 cycles are shown in Fig. S7. The increase of surfactant concentration leads to a significant increase in V_A for solutions without AF, whereas in the presence of AF, PVA 18–88 concentration has no effect on V_A. Similar effect is observed also for Brij 35 after 10 cycles, while the foamability of Brij solution starts to increase with C_S after 100 and 1000 cycles. For SLES the foamability increases with C_S even after 10 cycles in the presence of 20 ppm AFE or AFD. This very different behavior demonstrates that the antifoam not only preserves its activity upon prolonged shaking in PVA solutions but also it is able to suppress the foamability of these solutions even of higher PVA concentrations. It is also seen that AFD is more efficient as compared to AFE to decrease the foamability of the solutions at all studied surfactant concentrations. The only exception is with SLES solution after 10 cycles where the results for AFE and AFD are very similar.

Antifoam efficiency, *AE* is shown as a function of surfactant concentration C_S after 10 and 1000 cycles in Fig. 3. As can be seen, *AE* remains close to 100% for PVA 18–88 with $C_S \leq 1$ g/L and starts to decrease with the further increase of C_S at 10 and 1000 shaking cycles. Antifoam efficiency is very high for Brij 35 solutions with $C_S \leq 0.1$ g/L and remains high even at 10 g/L after 10 shaking cycles, while almost linear decrease of *AE* with lgC_S is observed for this surfactant after 1000 cycles. The lowest *AE* is determined again for SLES under all conditions studied and, for example, the antifoam cannot destroy the foam and *AE* decreases down to 5% at $C_S = 10$ g/L and prolonged agitation.

From this series of experiments, we can conclude that the efficiency of antifoam is the lowest with respect to SLES stabilized foam in the entire range of surfactant (between 0.1 and 10 g/L) and antifoam (between 2 and 200 ppm) concentrations. Intermediate efficiency is determined with respect to Brij 35, followed by higher efficiency with respect to PVA with 88% DH and very high efficiency with respect to PVA with 98% DH. The antifoam is more effective when it is introduced as dispersion in TXIB as compared to the emulsified antifoam. The latter effect is especially significant for Brij 35 and PVA solutions with 88% DH whereAFE has 2-fold lower antifoam efficiency as compared to AFD The increase in surfactant concentration leads to lower AF efficiency, whereas the increase of AF concentration increases *AE* significantly. The number of shaking cycles has significant effect on *AE* for low molecular mass surfactants (SLES and Brij 35) and almost no effect for PVA solutions. For PVA solutions the PVA concentration also has much smaller effect, as compared to its effect for the low molecular mass surfactants (SLES and Brij 35).

4.2. Shake test

The effect of AF concentration on *AE* at $C_S = 5$ g/L in shake test was studied. In this test *AE* remains almost constant as a function of the shaking cycles, which means that there is no significant exhaustion of the antifoam in this test. Note that in this test the ratio between the antifoam quantity and the maximal foam volume is ≈ 6.3 times higher as compared to Bartsch test, because the solution volume is 2-times larger (20 vs 10 ml) and the maximal foam volume is around 3-times smaller (30 vs 95 ml). The size of formed bubbles is very similar in these two tests, and as a consequence, the probability for entrapment of active antifoam globules is around 6-times higher in this test. Therefore, the exhaustion of the antifoam is not very pronounced in this test. The obtained data for *AE* as a function of antifoam concentration for AFD

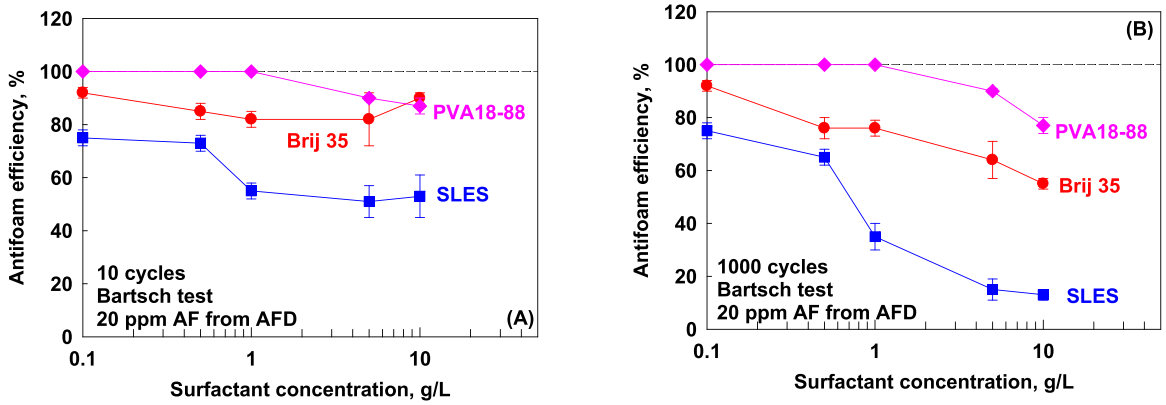

Fig. 3. Antifoam efficiency, *AE*, as a function of surfactant concentration for foams formed after (A) 10 and (B) 1000 cycles in Bartsch test for antifoam dosed as AFD in solution of SLES (blue squares); Brij 35 (red circles); PVA 18–88 (pink diamonds); PVA 10–98 (green triangles).

and AFE is shown in Fig. 4. The trends obtained in this test are very similar to those obtained in Bartsch test – *AE* increases almost linearly with lgC_{AF}. For PVA with 98% DH, the presence of 2 ppm AFD is sufficient to prevent the air entrapment. The value of *AE* for PVA with 88% DH are very similar for all PVA samples with different molecular masses and it increases from 70% at $C_{AF} = 2$ ppm up to 100% at 200 ppm AFD. Lower values of *AE* are determined for Brij 35, as compared to PVA with 88% DH, which is also the case for foams generated in Bartsch test after 1000 cycles. In the shake test AFE is less efficient as compared to AFD, especially for sterically stabilized foams (PVA and Brij 35), whereas the efficiency of AFE is somewhat higher as compared to AFD for SLES stabilized foams at low C_{AF}.

We conclude that the main trends observed in Bartsch test are observed also in the shake test.

4.3. Ultra Turrax

The effect of AF concentration for foams formed in UT at $C_S = 5$ g/L was also studied, see Fig. 5. The foamability of SLES solution remains unaffected even after introducing 2000 ppm of AFD or AFE in the foaming solution. Note that in this test the maximal AF concentration is 10-times higher as compared to the maximal AF concentration tested in shake and Bartsch tests – nevertheless, even AFD is unable to affect the foamability of 5 g/L SLES solution. Therefore, the studied antifoam is much less efficient with respect to foams generated in UT, as compared to foams formed in the shake and Bartsch tests when SLES is used as foam stabilizer.

Very low efficiency of the studied antifoam is determined also for foams formed in UT from solutions of 5 g/L Brij 35 and PVA with 88% DH. More than 10-times higher AF concentration is required in this test, as compared to shake and Bartsch tests, for noticeable antifoam action with respect to those solutions. Good antifoam efficiency is determined for AFD in PVA solutions with 98% DH, where 20 ppm AF suppresses completely the foamability of these solutions.

The efficiency of AFE in this test is very low at $C_{AF} \leq 20$ ppm for all studied surfactant and PVA solutions, even for PVA with 98% DH. Significant difference in the efficiency of antifoam is seen at $C_{AF} = 200$ ppm where AFE suppresses completely the foamability of PVA with 98% DH, while it has no effect for SLES solutions. Therefore, at higher antifoam concentrations, the rating of the surfactants in this test becomes similar to the rating in the other tests: the foam of SLES is the most stable one, intermediate stability is determined for Brij 35 and PVA with 88%, and the lowest stability for PVA with 98% DH. However, the concentrations of AF required to induce drop in foamability depend significantly on the foaming test.

The effect of surfactant concentration was studied at $C_{AF} = 20$ ppm, see Fig. 6. There is a threshold surfactant concentration below which the AF pre-dispersed in TXIB is able to suppress the foamability of the solutions studied. This concentration is the lowest for SLES foams, intermediate for Brij 35, higher for PVA 18–88 and the highest for PVA 4–98. Interestingly, when AFE is added to the surfactant solution, even at the lowest studied surfactant concentration, the AFE is unable to prevent the foamability of SLES, Brij 35 and PVA 18–88. Emulsified AF is able to suppress only the foamability in PVA 4–98 solutions of low concentrations, see Fig. 6B.

4.4. Comparison of antifoam efficiency in the different foaming tests

The obtained results clearly show that the studied antifoams have similar effect on PVA solutions with fixed DH and different molecular weights. In the three foaming tests, the results for PVA 4–88; PVA 8–88; PVA 18–88 and PVA 40–88 are very similar to each other and the results for PVA 4–98 and PVA 10–98 are also very similar. This means that the molecular weight has no significant impact on the AF action. Note that in our previous study [44] we showed that the surface tension isotherms and dynamic surface properties do not depend on the molecular mass of the PVAs at a given DH, which explain why we do not see any significant difference in the performance of the studied antifoam with respect to PVA solutions with different molecular masses.

To compare the efficiency of the studied antifoam dispersion and antifoam emulsions, we plotted the values of *AE* vs the ratio of antifoam to surfactant concentrations for PVA18–88; PVA 4–98; SLES and Brij 35 after longest shaking or mixing time (1000 cycles for Bartsch and shake tests, and 120 s for UT) in Fig. 7. One sees that the experimental data from the two series of experiments (fixed C_{AF} and varying C_S; fixed C_S and varying C_{AF}) lay on the same curve when the data are plotted as a function of C_{AF}/C_S, showing that higher AF concentration is required to destroy the foams formed from solutions with higher surfactant concentration. The experimental results for the antifoam efficiency for Bartsch and shake tests are very similar for SLES, PVA 18–88 and PVA 10–98, whereas for Brij 35 at low C_{AF}/C_S much better antifoam efficiency is determined for foams formed in Bartsch test, as compared to those in shake test. The lowest antifoam efficiency at a given C_{AF}/C_S, is obtained for foams formed in UT when SLES, Brij35 and PVA 18–88 are used.

From this comparison we conclude that the antifoam efficiency is much higher in the foaming tests in which the foam generation is related to the liquid splashing and it is characterized with significant bubble area expansion thus facilitating the entrapment of active antifoam globules between the relatively large bubbles. Note that in these tests the characteristic time for surfactant adsorption is shorter, as compared to Ultra Turrax method. In the latter test, there is no liquid splashing and a

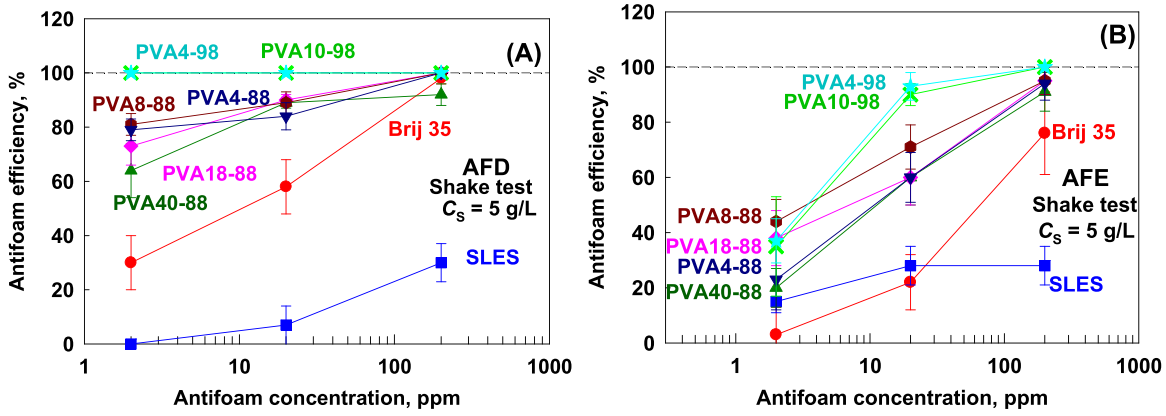

Fig. 4. Antifoam efficiency, *AE*, to destroy the foam generated in shake test from 5 g/L solutions of SLES (blue squares); Brij 35 (red circles); PVA 40–88 (green triangles up); PVA 18–88 (pink diamonds); PVA 8–88 (brawn hexagons); PVA 4–88 (blue triangles down); PVA 10–98 (green stars) and PVA 4–98 (cyan X) for antifoam added as (A) antifoam dispersion and (B) antifoam emulsion.

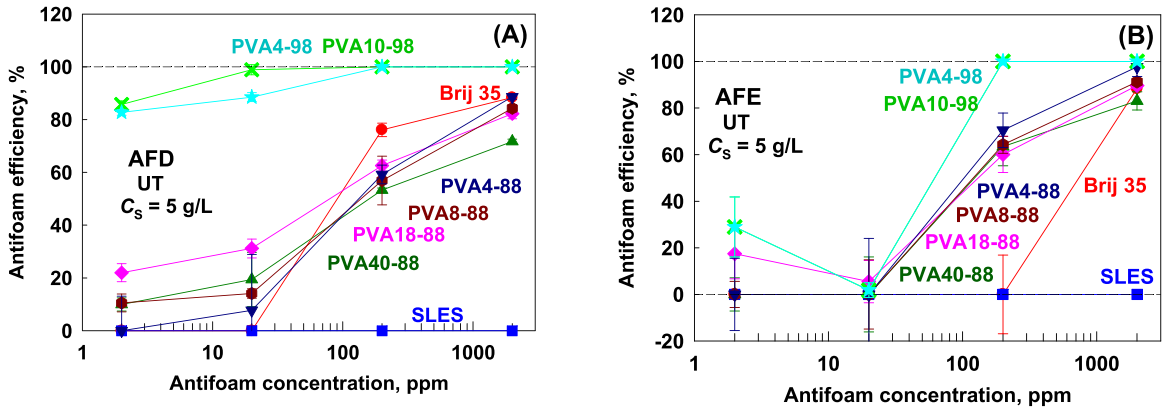

Fig. 5. Antifoam efficiency, *AE*, to destroy the foam generated in UT from 5 g/L solutions of SLES (blue squares); Brij 35 (red circles); PVA 40–88 (green triangles up); PVA 18–88 (pink diamonds); PVA 8–88 (brawn hexagons); PVA 4–88 (blue triangles down); PVA 10–98 (green stars) and PVA 4–98 (cyan X) for antifoam added as (A) antifoam dispersion and (B) antifoam emulsion.

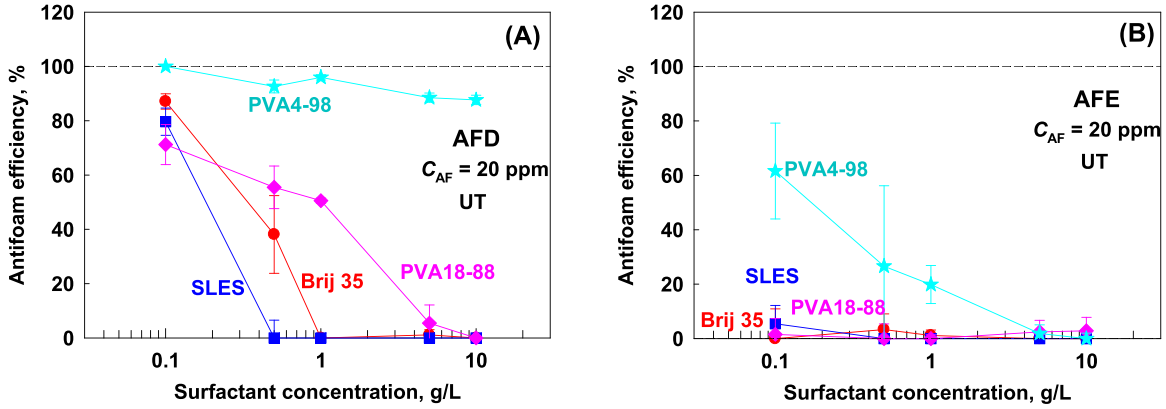

Fig. 6. Antifoam efficiency, *AE*, as a function of surfactant concentration for foams formed in UT from SLES (blue squares); Brij 35 (red circles); PVA 18–88 (pink diamonds); PVA 4–98 (cyan stars) solutions in presence of 20 ppm AF introduced as (A) antifoam dispersion and (B) antifoam emulsion.

significant fraction of the antifoam globules remain in the aqueous solution. The characteristic time for adsorption of surfactant on the bubble surface is longer in UT method and the adsorption layers are much closer to the equilibrium ones, thus increasing the stability of the pseudo emulsion films formed between the antifoam globules and the bubble surface. Also, the smaller bubbles in UT decrease the probability for entrapment of active antifoam globules in foam films.

From all these experiments we can conclude that the rate of foam generation has very significant impact on the antifoam efficiency for all studied surfactants – the effect is the highest for PVA with 88% DH and Brij 35 solutions, for which the antifoam is very efficient in the methods with significant expansion of the surface area during foam generation (Bartsch and shake tests) and AF is much less effective when smaller bubbles with low rate of surface expansion are formed in Ultra Turrax method.

5. Model experiments

5.1. Spreading ability of the studied AF dispersion and AF emulsion

To determine the mechanism of AF action with respect to the studied surfactant and polymer solutions, we performed a series of experiments in which the spreading ability of AFD and AFE over the solution surface was studied by measuring the solution surface tension and by observing the process of spreading under an optical microscope.

The experimental data from spreading measured by Wilhelmy plate method are shown in Fig. 8 and S8. One sees that the studied antifoam is able to spread over the solution surfaces and to decrease the surface tension for all studied surfactants and PVA solutions. Interestingly when the antifoam dispersion is spread the final surface tension differs for different surfactants and PVA solutions, whereas when antifoam emulsion is used, the final surface tension after spreading is the same for all studied surfactants and PVA solutions. This difference is related to the presence of TXIB in the antifoam dispersion which changes the properties of the adsorption layer, depending on the surfactant used, because TXIB is an organic solvent that can change the interactions between the adsorbed molecules. In the case of antifoam emulsion spreading the antifoam spreads over the surfactant tails and the surface tension is controlled mostly by the surface tension of the spread oil used for antifoam preparation. The drop in surface tension after the AF spreading is calculated from the difference between the surface tensions measured 10 s before and after AF spreading. The determined surface tension difference is shown in Fig. 8. As a rule, the emulsion spreading leads to bigger change in the surface tension, as compared to the antifoam dispersion. The highest change in surface tension is measured for PVA solutions with 98% DH for which the studied AF has the highest ability to suppress their foaming. An intermediate change in surface tension is measured for PVA solutions with 88% DH. The smallest decrease is determined for SLES and Brij 35 solutions. The difference in surface tension before and after spreading indicates that the used AF affects very significantly the adsorption layer of PVA with 98% DH by disturbing it and thus facilitates its efficiency to induce the coalescence between the bubbles during foam generation.

The process of AF spreading was observed under an optical

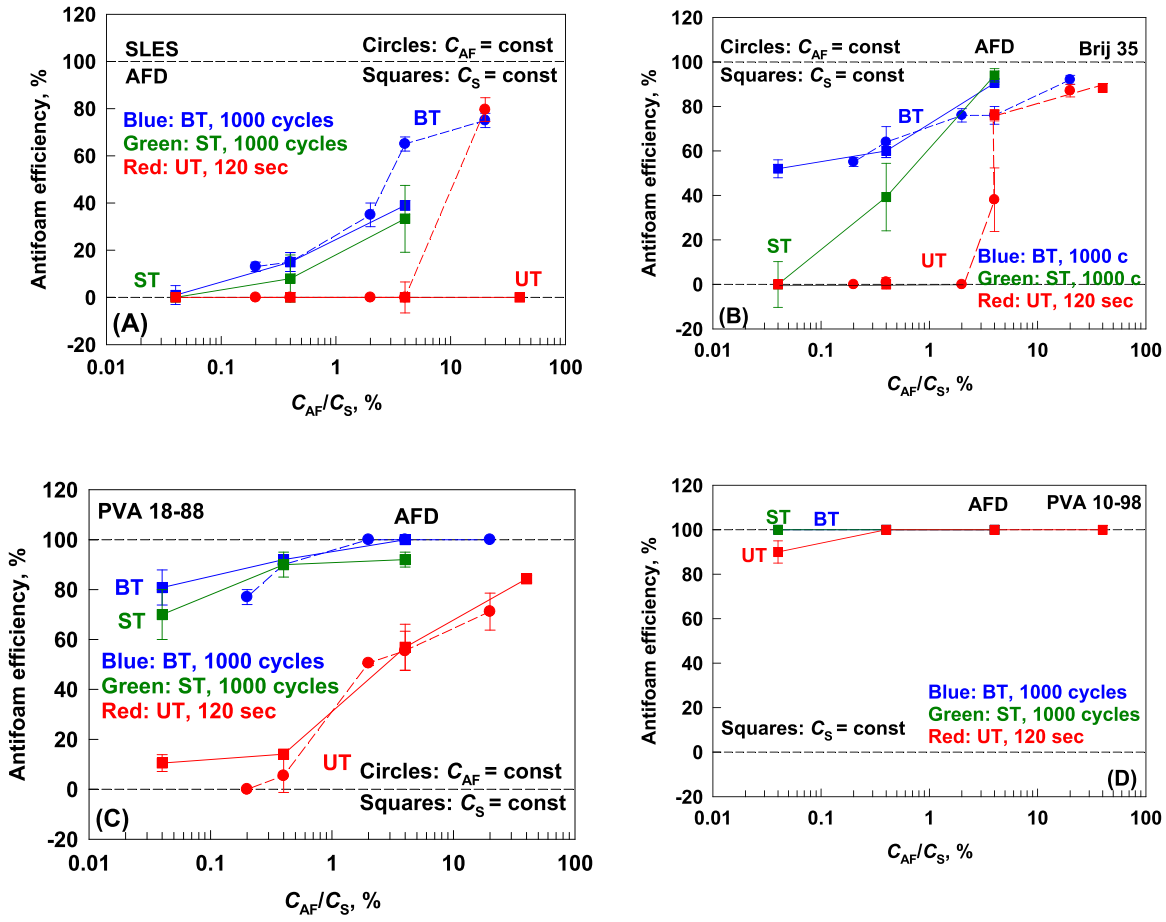

Fig. 7. Antifoam efficiency as a function of the ratio between the antifoam and surfactant concentrations for foams formed in Bartsch test (blue symbols); shake test (green symbols); Ultra Turrax (red symbols) from (A) SLES; (B) Brij 35; (C) PVA 18–88 and (D) PVA 10–98 solutions. The squares show the results from series in which the antifoam concentration is changed at fixed surfactant concentration, whereas the circles show the experimental data obtained at fixed antifoam concentration and different surfactant concentrations.

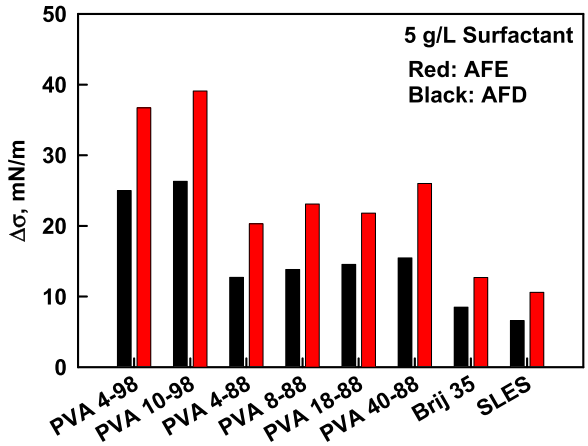

Fig. 8. Change in surface tension after spreading of AFD (black) and AFE (red) for different surfactant and PVA solutions. The surfactant concentration is 5 g/L.

microscope in reflected light. The initial spreading on PVA solution surfaces leads to the formation of a thick spread layer in equilibrium with oil lenses containing silica particles – see the illustrative images in Fig. 9 for PVA solutions. These lenses are evenly distributed on the solution surface and when two lenses come close to each other they merge and form one bigger lens which leads to some decrease in the number of oily lenses over time. The process of AFD spreading on Brij 35 solution is similar to that observed for PVA solutions in its initial stages – thick spread layer with many oil lenses are formed after placing the AFD on the solution surface. The evolution of the process is somewhat different. For PVA solutions the spread layer remains thick for at least 2 min, whereas the layer formed on Brij 35 surface gradually thins down and after 2 min it becomes with thickness below 30 nm, see the image in Fig. 9. The rate of thinning of the oily layer that spreads on SLES surface is much faster, as compared to Brij 35. After 1 min very thin spread layer is formed and the contact angle of the oily lenses that contain silica particles is very different when compared to the contact angle for Brij 35 and PVA solutions. As seen from the images shown in Fig. 9, these contact angles are very small for Brij 35 and PVA solutions and, that is why, interference fringes are well seen around the silica particles. In the case of SLES, there is a significant coalescence between the oily lenses and increase in the contact angle of these lenses with time. The thickness of the formed spread layer has significant impact on the efficiency and exhaustion of antifoam. Thick layer facilitates formation of drops with particles in them after film rupture, whereas the breakage of thin layer leads to faster segregation of silica-free and silica-enriched antifoam globules both of them being inactive in SLES foams, see Fig. S11. The spreading pattern explains why the AF gradually lost its efficiency in SLES and Brij 35 solutions in the course of foam destruction, see Fig. S2E, whereas it stays active even after 1000 shaking cycles in PVA solutions, see Fig. S2C.

The process of AFE spreading on the solution surfaces was also studied. Illustrative images are shown in Fig. 9 (lower row). During AFD

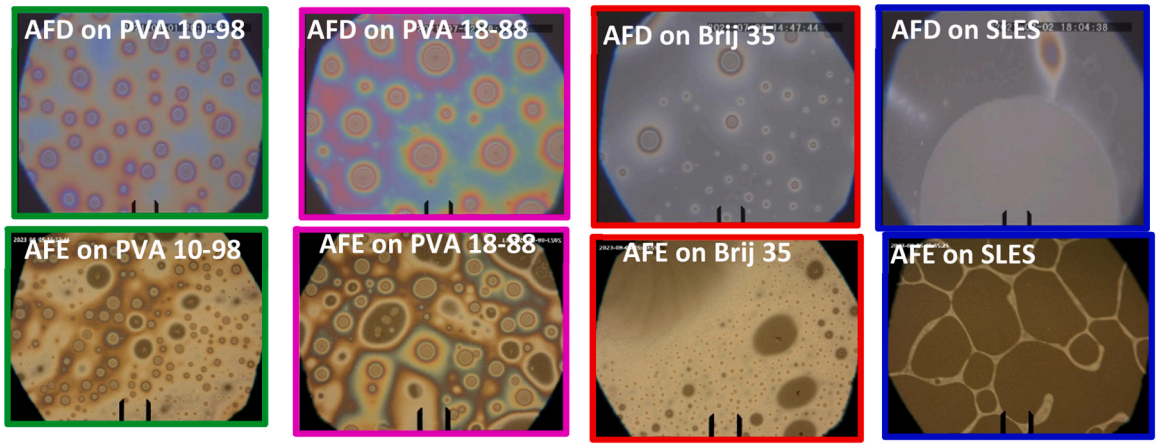

Fig. 9. Illustrative pictures of solution-air interface after spreading of AFD (first row) and AFE (second row) on solution surface. All solutions contain 5 g/L surfactant or polymer.

spreading, evenly distributed oil lenses are observed on PVA solution surface, whereas during AFE spreading solid segregated particles surrounded by thin oil layer are frequently observed along with oil lenses with relatively small contact angle that are surrounded by thick oil layer. These solid particles are probably some of the particles that have been in contact with emulsifiers during the emulsification process and their wettability from the silicone oil used for antifoam preparation has been changed. The fraction of these particles is not negligible and probably they are the reason for the lower activity of AFE as compared to AFD. The spreading of AFE on Brij 35 solution also shows the presence of many phase separated particles, surrounded by thin layer. In the case of SLES, the spread layer thins down very quickly to very small thickness and the silicone oil forms interesting network on the solution surface. This network is unstable, it breaks and forms very small oil lenses which, however, in most cases do not contain silica particles. From these observations we can conclude that the surfactant used has significant impact on the mode of AF spreading. Low molecular mass surfactants facilitate the formation of thin spread oil layer which during foam film rupture forms numerous small oily drops which are unable to enter the bubble surface and, as a consequence, the antifoam efficiency is lost.

All these observations are performed by spreading of AFD or AFE over 5 g/L surfactant or PVA solution surface. In our previous studies, we showed that during the foaming process part of the initially spread antifoam is emulsified as oily drops in the solution and when their entry barrier is high, these drops cannot enter the solution surface again and the foamability of the solution is restored, viz. AF is deactivated. To check whether the studied antifoam is able to enter the solution surface during the foam generation we measure the surface tension of the solutions that are shaken different numbers of cycles in Bartsch test. The obtained results showed that $\Delta\sigma$ decreases from 6.3 mN/m (immediately after spreading) to 1 mN/m after 1000 shaking cycles for SLES, showing that only a very tiny fraction of the AF is able to enter the solution surface and to induce bubble-bubble coalescence after prolonged shaking. Significant reduction in $\Delta\sigma$ is measured also for Brij 35 solution for which the initial value of $\Delta\sigma \approx 9.7$ mN/m decreases down to $\Delta\sigma \approx 4.3$ mN/m after 1000 cycles. Part of the AF placed on PVA 18–88 solution is also emulsified during foaming and $\Delta\sigma$ decreases from 14 mN/m down to 7 mN/m. From these measurements we can conclude that the spreading and entering of the emulsified drops is most difficult for SLES solutions, intermediate for Brij 35, and easiest for PVA 18–88. Similar conclusions can be drawn from the optical observations made after 1000 cycles shown in Fig. S9 - it is seen that oily lenses are frequently seen on PVA 18–88 surface, whereas only very thin spread layer remains on SLES surface.

5.2. Stability of horizontal and vertical foam films

The behavior of vertical foam films, formed from 5 g/L SLES, Brij 35 and PVA 18–88 solutions in presence of 200 ppm AF, was studied. The solutions contain a lot of AF globules which can induce the film breakage. Therefore, all foam films were very unstable and ruptured within 1 s after the film formation. These results illustrate the fact that the studied antifoam is very active when the AF globules are entrapped in the film interior and the film surfaces rapidly expands as in this experiment. Note that under these conditions the antifoam is very active with respect to foams generated in Bartsch and shake tests, where significant surface expansion occurs during foaming.

The stability of horizontal foam films, formed in capillary cell, was also studied. Note that the area of the horizontal films is much smaller, as compared to that of the vertical films (0.1 vs 100 mm^2) which corresponds to significantly lower probability for antifoam entrapment in the foam films. Another difference between the horizontal and vertical films is the smaller surface expansion for the horizontal films. The stability of the horizontal films, formed from solutions containing 200 ppm AF which have been shaken 10 cycles in Bartsch test, was very low despite the smaller area of the foam films and the milder conditions during film generation, which demonstrates the high initial activity of the antifoam. When the foam films are formed from solutions which have been shaken 1000 cycles in Bartsch test, the situation is different. The number of oil lenses on the solution surface is much lower and the probability for entrapment of oil lens that is able to break the foam film is much lower. As a consequence, the foam films formed from SLES solution, at this high AF concentration, remain stable and thin down to their equilibrium thickness. Fraction of the films formed from Brij 35 solutions also remain stable, but 30% of them breaks during their thinning due to the entrapment of antifoam globules. Most of the films formed from PVA 18–88 break in the course of their thinning, because they entrap larger number of antifoam globules as compared to the low-molecular mass surfactants. The slower thinning of PVA 18–88 films facilitates the antifoam action giving longer time for formation of unstable oil bridges from entrapped antifoam globules. The experimental results for the probability for film rupture are shown in Fig. 10. The obtained results are in a very good qualitative agreement with the results obtained in the foaming tests.

6. Discussion

The efficiency of dynamic antifoams depends on the probabilities for (1) Entrapment of antifoam globules in the foam film formed between two neighboring bubbles during foaming; (2) Rupture of the pseudo-emulsion films between the antifoam globules and the bubble surfaces

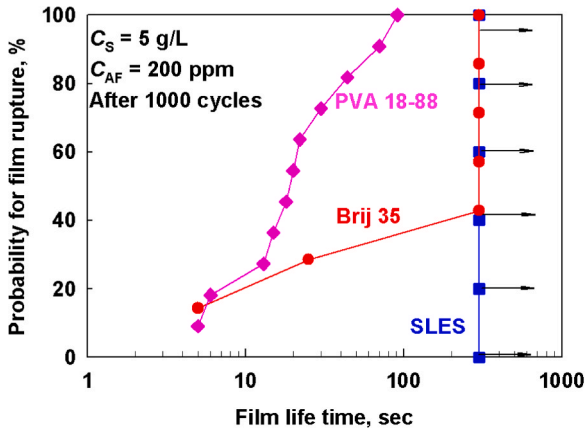

Fig. 10. Probability for film rupture after certain period of time for films formed in capillary cell from 5 g/L PVA 18–88 (pink diamonds); Brij 35 (red circles); SLES (blue squares) solutions containing 200 ppm AF, dosed as AFD, which have been shaken 1000 cycles in Bartsch test. The arrows show that the film life time is longer than 300 s, which is the longest time during which the films were observed.

which results in formation of oil bridges in the foam films; (3) Rupture of the oil bridges which leads to coalescence of two neighboring bubbles. The first process significantly depends on the concentration of antifoam globules in the foaming solution and the size of the bubbles which controls the area of the foam films formed between them. The second process depends on the stability of the film formed between the antifoam globules and the air-water interface (so-called entry barrier), which in its own turns depends on the type of stabilizer used for foam generation, rate of surfactant adsorption, rate of film thinning, presence of spread oil layer on the solution surface. The third process depends mainly on the properties of the used antifoam and slightly depends on the conditions for foam generation and used foam stabilizers. Therefore, the factors studied in the current study can be explained by their effect on the first two processes.

As seen from the data obtained in different foaming tests and for different foam stabilizers, the increase of antifoam concentration at fixed surfactant concentration increases the antifoam efficiency, which can be explained by the increased probability for entrapment of antifoam globules in the foam film during foaming.

The much higher antifoam efficiency in Bartsch and shake tests, as compared to Ultra Turrax is related to: (1) Lower probability for entrapment of antifoam globules in foam films formed between smaller bubbles in UT, as compared to the other two methods, and (2) Lower probability for destabilization of the films formed between the antifoam globules and the air-water interfaces, because of the longer adsorption time in UT which facilitates the formation of adsorption layers with almost equilibrium properties. The shorter time for surfactant adsorption accompanied with larger stretching of the film area in Bartsch and shake tests leads to lower surfactant adsorption and facilitated antifoam efficiency.

The different performance of the antifoam in the studied solutions for given foaming test is related to the different stability of the pseudo-emulsion films, formed between the antifoam globules and the air-water interface, see Fig. 11. When PVA with 98% DH is used, the rate of PVA adsorption is low and the formed adsorption layers are loose due to the high hydrophilicity of these PVA molecules. As a consequence, the dynamic and equilibrium surface tensions are very high (> 60 mN/m), the equilibrium adsorption is low (< 1 mg/m^2), and the stability of the antifoam globule-water-air film is low, which facilitates the formation of oily bridges between the foam film surfaces. For that reasons, the efficiency of all antifoams is very high to foams formed from PVA with 98% DH.

The presence of 12% acetate groups in PVA molecules with 88% DH increases significantly their adsorption ability and decreases the

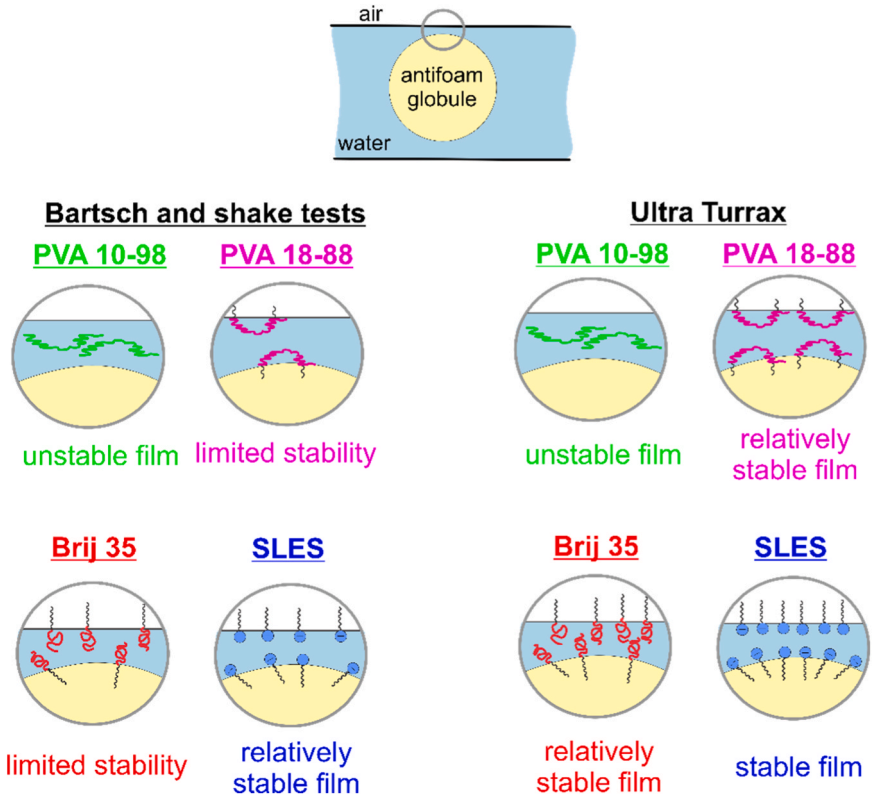

Fig. 11. Schematic representation of the films formed between the antifoam globules and the air-water interface in the fast and slow foaming methods, for the different surfactant and PVA solutions.

dynamic and equilibrium surface tensions [44]. As a consequence, the stability of the pseudo-emulsion films increases, as compared to PVA with 98% DH, and starts to depend on the characteristic time for foam generation. The antifoam is very active in foams formed from PVA solutions with 88% DH in Bartsch and shake tests, where the polymer molecules have no sufficient time to form equilibrium adsorption layers, while being less efficient in Ultra Turrax where longer adsorption time leads to formation of adsorption layers with almost equilibrium properties, see Fig. 11. It has to be noted that the long ranged steric repulsion which was found to increase the foamability at instantaneous surface coverage of 80% in the absence of antifoams [44] are unable to prevent the antifoam action of the studied antifoam because the spread oil changes the equilibrium adsorption of these PVA molecules. The lower efficiency of the antifoam in UT is related to the longer time for PVA adsorption and the creation of the effective entry barrier which suppresses the formation of oily bridges in the foam films. The slow thinning of the spread oil layer decreases the rate of segregation of the silicone oil and silica particles, thus maintaining the high efficiency of the antifoam upon prolonged foaming.

The initial antifoam activity (after 10 cycles) with respect to Brij 35 foams in Bartsch test is very similar to that for PVA with 88% DH, because of the relatively slow adsorption of Brij 35 molecules for which the surface coverage has to be $> 95\%$ [44] to ensure stabilization of the foam films without antifoams. The main difference between Brij 35 and PVA 88% DH is related to the fact that the antifoam efficiency decreases upon foam generation for Brij 35 and does not change for PVA 88% DH which is related to the antifoam exhaustion (due to segregation of silica particles and silicone oil in Brij 35). The latter effect correlates very well with the significant thinning of the spread oil layer over time which boosts the formation of small oily drops free of silica particles which have limited activity, see Fig. S11.

The presence of electrostatic repulsion between the film surfaces when SLES is used as foam stabilizer leads to stabilization not only of the foam films without antifoam at low surface coverage, but also of the films formed between the antifoam globules and air-water interface (high entry barrier). The faster surfactant adsorption and the lower surface coverage required for film stabilization explains the much lower antifoam efficiency with respect to SLES foams, see Fig. 11. Fast thinning of the spread oil layer on the solution-air interface facilitates the segregation of the silicone oil and the silica particles and leads to loss of antifoam efficiency during prolonged foaming. The longer adsorption time with the smaller probability for entrapment of antifoam globules in the foam films reduces the antifoam activity in foams formed from SLES solutions in UT.

The efficiency of antifoam emulsion is much lower as compared to antifoam dispersion for the studied systems (except for SLES) which is explained with the easier segregation of the silica particles and the silicone oils as seen from the optical observations of the spreading process. The presence of nonionic surfactants in the emulsions facilitates the formation of mixed adsorption layers on the antifoam globule surface and increases the stability of the pseudo-emulsion films. The worse performance of the antifoam emulsion, as compared to the antifoam dispersion, is very pronounced in UT test where there is a sufficient time for creation of dense adsorption layer and the probability for entrapment of antifoam globules in the film interior is smaller due to smaller bubble size.

To determine whether the ability of the surfactant to prevent the antifoam action depends on the surface properties of the air-water interface, we plotted the antifoam efficiency as a function of the different properties of the dynamic adsorption layers. The dependences of *AE* at 20 ppm antifoam, as a function of dynamic surface tension and dynamic surface coverage, for foams formed in Bartsch test, are compared in Fig. S10. One sees that, at the same dynamic surface coverage, better antifoam efficiency is determined for the sterically stabilized foams, as compared to electrostatically stabilized foams. The latter observation evidences that, even in presence of antifoam, the electrostatic repulsion between the bubble surfaces has significant impact on the foam stabilization.

7. Conclusions

The efficiency of mixed functionalized PDMS-silica antifoam was studied with respect to anionic (SLES), nonionic (Brij 35), and PVA solutions with two different degrees of hydrolysis (98% and 88%) and different molecular weights (between 31 and 205 kDa) in three foaming methods (Bartsch test, shake test and Ultra Turrax). Experiments were performed at different antifoam and surfactant concentrations by using antifoam pre-dispersed in organic solvent (TXIB) or emulsified as antifoam-in-water emulsion. The main conclusions can be summarized as follows:

(1) The antifoam efficiency increases with the ratio of antifoam to surfactant concentrations in a given test, due to the higher probability for entrapment of antifoam globule able to break the foam films at higher antifoam concentration and lower entry barrier at lower surfactant concentration.
(2) The studied antifoam is more efficient when it is introduced as antifoam dispersion as compared to antifoam emulsion, which is related to the easier segregation of the silica particles and silicone oil when the antifoam emulsion is used (i.e. faster antifoam exhaustion).
(3) The antifoam is very efficient to prevent the foam generation in PVA solutions with 98% DH, it has intermediate efficiency with respect to foams stabilized by PVA with 88% DH and Brij 35, and it is least efficient with respect to SLES foams. The presence of electrostatic repulsion in SLES foams increases the entry barrier of the antifoam globules and decreases the antifoam ability to induce coalescence of the formed bubbles (i.e. higher entry barrier). Lower stability of foams formed from PVA with 98% DH is explained with the lower PVA adsorption and the larger effect of antifoam on the PVA adsorption layer after its spreading on the bubble interface.
(4) At a certain degree of hydrolysis, the molecular mass of PVA has no significant effect on the antifoam activity which is due to very similar surface and film properties of PVA samples with different masses as shown in Ref. [44].
(5) The antifoam efficiency decreases upon prolonged foaming in Bartsch test for SLES and Brij 35 stabilized foams, due to the segregation of the silica particles and silicone oil upon foam film which is related to the formation of thin spread layer of the oil in contact with silica particles aggregates after spreading of the antifoam on the solution surface. The activity of the antifoam remains unaffected during foaming with respect to PVA foams, because the antifoam spreads as a thick layer which decreases the rate of silica-silicone oil segregation.
(6) The studied antifoam is much more efficient in the foaming tests in which the air entrapment is accompanied with significant surface expansion of the bubble surface (such as Bartsch and shake tests) and much less efficient in Ultra Turrax in which the bubbles are smaller and have much more time for formation of equilibrium adsorption layer on their surface before colliding with each other.

In the current study for first time we showed that the antifoam efficiency depends on the type of forces that are operative for foam stabilization – the antifoam is much more efficient for sterically stabilized foams and much less efficient for electrostatically stabilized foams with small bubbles.

Funding

This work was supported by Altana Institute, Germany and by

Operational Program “Science and Education for Smart Growth” 2014–2020, co-financed by European Union through the European Structural and Investment Funds, Grant BG05M2OP001–1.002–0012 “Sustainable utilization of bio-resources and waste of medicinal and aromatic plants for innovative bioactive products”.

CRediT authorship contribution statement

Vassil Georgiev: Investigation, Formal analysis, Visualization, **Zlatina Mitrinova:** Formal analysis, Writing – Original draft. **Alexander Gers-Barlag**: Conceptualization; Funding acquisition; **Guillaume Jaunky:** Conceptualization; Funding acquisition **Nikolai Denkov**: Conceptualization, Methodology, Funding acquisition. **Slavka Tcholakova**: Conceptualization, Methodology, Formal analysis, Writing – Review & Editing, Supervision.

Declaration of Competing Interest

The authors declare that they have no known competing financial interests or personal relationships that could have appeared to influence the work reported in this paper.

Data availability

Data will be made available on request.

Appendix A. Supporting information

Supplementary data associated with this article can be found in the online version at doi:10.1016/j.colsurfa.2023.132838.

References

[1] G. Zocchi, Foam in Consumer Products in *Handbook of Detergents,* Part A*: Properties*, Ed. Guy Broze, CRC Press, Boca Raton, 1999. Chapter 10.
[2] J. Payne, M. Talavera, K. Koppel, Consumer perceptions of hotel shampoos and lotions, J. Sens. Stud. 38 (3) (2023), e12817.
[3] E.L. Roberto, Perceived product attributes, consumer motivaton and product positioning decisions, Philippine review of economics, Univ. Philipp. Sch. Econ. Philipp. Econ. Soc. 16 (3&4) (1979) 117–130.
[4] C.J. Thompson, N. Ainger, P. Starck, O.O. Mykhaylyk, A.J. Ryan, Shampoo science: a review of the physiochemical processes behind the function of a shampoo, Macromol. Chem. Phys. 224 (2023) 2200420.
[5] Y. An, Y. Tian, C. Wei, Y. Tao, B. Xi, S. Xiong, J. Feng, Y. Qian, Dealloying: an effective method for scalable fabrication of 0D, 1D, 2D, 3D materials and its application in energy storage, Nanotoday 37 (2021), 101094.
[6] K. Zeng, D. Zhang, Recent progress in alkaline water electrolysis for hydrogen production and applications, Prog. Energy Combust. Sci. 36 (2010) 307–326.
[7] A. Lucas, C. Zakri, M. Maugey, M. Pasquali, P. van der Schoot, P. Poulin, Kinetics of nanotube and microfiber scission under sonication, J. Phys. Chem. C. 113 (48) (2009) 20599–20605.
[8] A. Hassan, K. Jumbri, A. Ramli, N. Borhan, Physio-chemical analysis of amide and amine poly(dimethylsiloxane)-modified defoamer for efficient oil-water separation, ACS Omega 6 (23) (2021) 14806–14818.
[9] A. Mahmoudkhani, L. Bava, B. Wilson, An innovative approach for laboratory evaluation of defoamers for oilfield cementing applications, Soc. Pet. Eng. - Braz. Offshore Conf. 2 (2011) 939–953.
[10] L. Bava, R. Wilson, Evaluation of defoamer chemistries for deepwater drilling and cementing applications, Soc. Pet. Eng. - SPE Deep. Drill. Complet. Conf. (2014) 590–600.
[11] I.C. Callaghan, Antifoams for nonaqueous systems in the oil industry, in: P. R. Garrett (Ed.), Defoaming: theory and industrial applications, Marcel Dekker, 1993.
[12] R. Farajzadeh, A. Andrianov, R. Krastev, G.J. Hirasaki, W.R. Rossen, Foam–oil interaction in porous media: implications for foam assisted enhanced oil recovery, Adv. Colloid Interface Sci. (1) (2012) 183–184.
[13] B. Junker, Foam and its mitigation in fermentation systems, Biotechnol. Prog. 23 (4) (2007) 767–784.
[14] A. Etoc, F. Delvigne, J.P. Lecomte, P. Thonart, Foam control in fermentation bioprocess: From simple aeration tests to bioreactor, Appl. Biochem. Biotechnol. 130 (1–3) (2006) 392–404.
[15] J.C. Nielsen, F.S.O. Lino, Th.G. Rasmussen, J. Thykær, C.T. Workman, T.O. Basso, Industrial antifoam agents impair ethanol fermentation and induce stress responses in yeast cells, Appl. Microbiol Biotechnol. 101 (2017) 8237–8248.
[16] R.E. Patterson, Influence of silica properties on performance of antifoams in pulp and paper applications. Nonwovens, Symp. . Notes Tech. Assoc. Pulp Pap. Ind. (1988) 39–48.
[17] E. Martorana, S. Kleemann, Influence of defoamers and deaerators on paper properties and process parameters, Prof. Papermak. 2 (2006) 26–31.
[18] S. Ando, The antifoams for pulp and paper industry - Defoaming technology in the pulp and paper industry, Kami Pa Gikyoshi/Jpn. Tappi J. 53 (9) (1999) 1126–1132.
[19] S.L. Allen, L.H. Allen, T.H. Flaherty, Defoaming in the pulp and paper industry, in: P.R. Garrett (Ed.), Defoaming: theory and industrial applications, Marcel Dekker, 1993.
[20] G.C. Sawicki, High performance antifoams for the textile dyeing industry, in: P. R. Garrett (Ed.), Defoaming: theory and industrial applications, Marcel Dekker, 1993.
[21] L. Gallez, Foam control for single-rinse fabric conditioners in Latin America, INFORM - International News on Fats, Oils Relat. Mater. 22 (2) (2011) 112–113.
[22] G.C. Sawicki, Impact of surfactant composition and surfactant structure on foam control performance, Colloids Surf. A 263 (1–3 SPEC. ISS.) (2005) 226–232.
[23] G. Saliholu, N.K. Salihoglu, A review on paint sludge from automotive industries: Generation, characteristics and management, J. Environ. Manag. 169 (2016) 223e235.
[24] K. Jo, M. Ishizuka, K. Shimabayashi, T. Ando, Development of new mineral oil-based antifoams containing size-controlled hydrophobic silica particles for gloss paints, J. Oleo Sci. 63 (12) (2014) 1303–1308.
[25] S.J. Storfer, J.T. DiPiazza, R.E. Moran, Advertorial - Bursting the bubble- foam killers, Colourage 54 (7) (2007) 93–96.
[26] R. Aveyard, B.P. Binks, P.D.I. Fletcher, T.G. Peck, C.E. Rutherford, Aspects of aqueous foam stability in the presence of hydrocarbon oils and solid particles, Adv. Colloid Interface Sci. 48 (C) (1994) 93–120.
[27] V. Bergeron, P. Cooper, C. Fischer, J. Giermanska-Kahn, D. Langevin, A. Pouchelon, Polydimethylsiloxane (PDMS)-based antifoams, Colloids Surf. A 122 (1–3) (1997) 103–120.
[28] A. Hilberer, S.-H. Chao, Antifoaming agents. Encyclopedia of Polymer Science and Technology, Wiley, 2012.
[29] P.R. Garrett, The science of defoaming theory. Experiment and Applications, CRC Press, Boca Raton, 2014.
[30] N.D. Denkov, Mechanisms of foam destruction by oil-based antifoams, Langmuir 20 (2004) 9463–9505.
[31] N. Denkov, S. Tcholakova, N. Politova-Brinkova, Physicochemical control of foam properties, Curr. Opin. Colloid Interface Sci. 50 (2020), 101376.
[32] N.D. Denkov, P. Cooper, J.-Y. Martin, Mechanisms of action of mixed solid–liquid antifoams. 1. Dynamics of foam film rupture, Langmuir 15 (1999) 8514–8529.
[33] A. Hadjiiski, N.D. Denkov, S. Tcholakova, I.B. Ivanov, Role of entry barriers in foam destruction by oil drops, in: K.L. Mittal, D.O. Shah (Eds.), "Adsorption and Aggregation of Surfactants in Solution", Marcel Dekker, New York, 2002, pp. 465–500.
[34] E.S. Basheva, D. Ganchev, N.D. Denkov, K. Kasuga, N. Satoh, K. Tsujii, Role of betaine as foam booster in the presence of silicone oil drops, Langmuir 16 (3) (2000) 1000–1013.
[35] N.D. Denkov, K.G. Marinova, S.S. Tcholakova, Mechanistic understanding of the modes of action of foam control agents, Adv. Colloid Interface Sci. 206 (2014) 57–67.
[36] N. Politova-Brinkova, M. Hristova, V. Georgiev, S. Tcholakova, N. Denkov, M. Grandl, F. Achenbach, Role of surfactant adsorption and surface properties for the efficiency of PDMS-silica antifoams, Colloids Surf. A 610 (2021), 125747.
[37] K.G. Marinova, N.D. Denkov, Foam destruction by solid-liquid antifoams in solutions of a nonionic surfactant: electrostatic interactions and dynamic effects, Langmuir 17 (2001) 2426–2436.
[38] K. Khristov, B. Jachimska, K. Malysa, D. Exerowa, Static’ and steady-state foams from ABA triblock copolymers: Influence of the type of foam films, Colloids Surf. A 186 (1–2) (2001) 93–101.
[39] D. Exerowa, R. Sedev, R. Ivanova, T. Kolarov, Th.F. Tadros, Colloids Surf. A 123–124 (1997) 277–282.
[40] D. Exerowa, T. Kolarov, I. Pigov, B. Levecke, T. Tadros, Langmuir 22 (11) (2006) 5013–5017.
[41] D. Langevin, Polyelectrolyte and surfactant mixed solutions. Behavior at surfaces and in thin films, Adv. Colloid Interface Sci. (2001) 467.
[42] N. Kristen, R. von Klitzing, Effect of polyelectrolyte/surfactant combinations on the stability of foam films, Soft Matter 6 (2010) 849.
[43] C. Uzum, N. Kristen, R. von Klitzing, Polyelectrolytes in thin liquid films, Curr. Opin. Colloid Interface Sci. 15 (2010) 303.
[44] V. Georgiev, Z. Mitrinova, N. Genchev, A. Gers-Barlag, G. Jaunky, N. Denkov, S. Tcholakova, Surface and foam properties of polyvinyl alcohol solutions, Colloids Surf. A In Press (2023), 132828 accepted,.
[45] T. Schuman, M. Wikstrom, M. Rigdahl, Coating of surface-modified papers with poly(vinyl alcohol), Surf. Coat. Technol. 183 (2004) 96–105.
[46] Z. Ling, C.E. Ren, M.-Q. Zhao, J. Yang, J.M. Giammarco, J. Qiu, M.W. Barsoum, Y. Gogotsi, Flexible and conductive MXene films and nanocomposites with high capacitance, PNAS 111 (47) (2014) 16676–16681.
[47] K. Jiang, S. Sun, L. Zhang, Y. Lu, A. Wu, C. Cai, H. Lin, Red, green, and blue luminescence by carbon dots: full-color emission tuning and multicolor cellular imaging, Angew. Chem. - Int. Ed. 54 (18) (2015) 5360–5363.
[48] X. Zhao, Q. Zhang, D. Chen, P. Lu, Macromolecules 43 (5) (2010) 2357–2363.
[49] M.I. Baker, S.P. Walsh, Z. Schwartz, B.D. Boyan, Journal Biomed. Mater. Res. - Part B Appl. Biomater. 100 (5) (2012) 1451–1457 (B).
[50] E.A. Kamoun, E.-R.S. Kenawy, X. Chen, J. Adv. Res. 8 (3) (2017) 217–233.

[51] B. Petkova, S. Tcholakova, M. Chenkova, K. Golemanov, N. Denkov, D. Thorley, S. Stoyanov, Foamability of aqueous solutions: role of surfactant type and concentration, Adv. Colloid Interface Sci. 276 (2020), 102084.
[52] B. Petkova, S. Tcholakova, N. Denkov, Foamability of surfactant solutions: interplay between adsorption and hydrodynamic conditions, Colloids Surf. A 626 (2021), 127009.
[53] A. Scheludko, Thin liquid films, Adv. Colloid Interface Sci. 1 (1967) 391–464.
[54] N.D. Denkov, K.G. Marinova, C. Christova, A. Hadjiiski, Ph Cooper, Mechanisms of action of mixed solid-liquid antifoams: 3. Exhaustion and reactivation, Langmuir 16 (2000) 2515–2528.